Diagonal time gating of stimulated photon echo

Pshenichnikov, Maxim S.; Boeij, Wim P. de; Wiersma, Douwe A.

Published in:
Summaries of Papers Presented at the Quantum Electronics and Laser Science Conference, 1996. QELS '96

of a quantum kinetic calculation that includes electron-electron scattering only, showing the time-evolution of the occupation number in k-space for excitation by a 20-fs pump pulse well above the band edge. The photocarriers rapidly scatter out of the energy window in which they were created. As a result of the memory, kinetic overshoots develop. We find indications of such overshoots also in the experimental data. A complete description of the DAS requires inclusion of the short coherent probe. We stress that a very short probe is *essential* for the observation of quantum-kinetic effects, which are due to the nonlocality of scattering. For a probe longer than the range of nonlocality (memory depth), >70 fs,

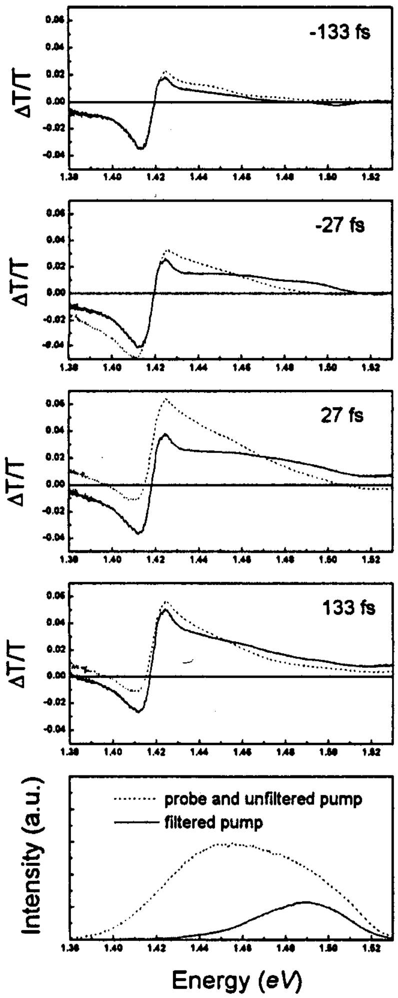

QThA2 Fig. 2 Spectrally resolved differential absorption signals measured with a 30-fs probe and two different pump durations: 100 fs (solid) and 30 fs (dashed). In both cases an immediate response is observed at the band edge. The bottom panel shows the spectrum of the 100-fs pump (solid) and that of the 30-fs probe/unfiltered pump (dashed).

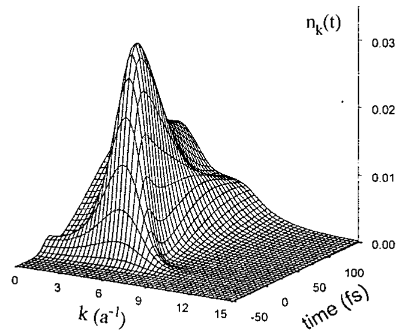

QThA2 Fig. 3 The time evolution of the occupation number in k-space after an excitation with a single 20-fs pump pulse, calculated in the framework of quantum kinetic theory.

the kinetics become indistinguishable from local Boltzmann kinetics.

Department of Physics, University of Florida at Gainesville

1. W. H. Knox, C. Hirlimann, D. A. B. Miller, J. Shah, D. S. Chemla, C. V. Shank, Phys. Rev. Lett. **56**, 1191 (1986).
2. S. M. Goodnick, P. Lugli, Phys. Rev. B **37**, 2578 (1988).
3. K. El-Sayed, L. Banyai, H. Haug, Phys. Rev. B **50**, 1541 (1994).
4. J.-P. Foing, D. Hulin, M. Joffre, M. K. Jackson, J.-L. Oudar, C. Tanguy, M. Combescot, Phys. Rev. Lett. **68**, 110 (1992).
5. M.-A. Mycek, J.-Y. Bigot, I. Perakis, D. S. Chemla, J. Nonlin. Opt. Phys. and Mat. **4**, 497 (1995).
6. A. Alexandrou, V. Berger, D. Hulin, Phys. Rev. B **52**, 4654 (1995).
7. A. V. Kuznetsov, Phys. Rev. B **44**, 8721 (1991) and Phys. Rev. B **44**, 13381 (1991).

QThA3 9:00 am

Diagonal time gating of stimulated photon echo: vibrational mode suppression in the non-Markovian limit

Maxim S. Pshenichnikov, Wim P. de Boeij, Douwe A. Wiersma, *Ultrafast Laser and Spectroscopy Laboratory, Department of Chemistry, Materials Science Centre, University of Groningen, Nijenborgh 4, 9747 AG Groningen, The Netherlands*

Numerous studies to date are devoted to a photon echo spectroscopy of a dissolved dye molecule. Because most dyes exhibit vibronic features in their absorption spectra for impulsive excitation, the initially excited state is a vibronic wave packet. Shank and coworkers were the first to recognize the importance of vibrational mode suppression toward optical dephasing measurements.[1] Mode suppression by *time-integrated* on a slow detector stimulated photon echo, however, works only in systems that exhibit Bloch-like dynamics, meaning that the echo peaks at the time equal to the delay between the first excitation pulses.

In this contribution we show that enhanced mode suppression can be obtained by time-gating the stimulated photon echo (SPE) at the conventional echo time and in phase with the wave packet dynamics. This novel technique is demonstrated on a dye solution of DTTCI in ethylene glycol. As it was directly shown recently, the dynamics of such a system is distinctly non-Markovian.[2] For the echo spectroscopy it means that the echo peaks at the times quite different from those prescribed by the Bloch model.

For the experimental realization of enhanced mode suppression we applied the phase-locked heterodyne detected stimulated photon echo.[3] In this technique,[4] (Fig. 1), three ultrashort pulses E_1, E_2, and E_3 induce a third-order polarization $P^{(3)}(t)$ on the optical transition. The resulting time-dependent signal field $E(t) \sim P^{(3)}(t)$ is interfered with a fourth replica pulse E_4. The heterodyne detected signal $S(t_{34}) \sim \mathrm{Re}[R^{(3)}(t)E_4^*(t_{34})]$ exceeds by far the one detected by time gating of the echo: $S \sim |P^{(3)}(t)|^2$.

To perform mode suppression experiments we first characterized the active vibrational modes. This information is obtained from a measurement of the so-called echo-maximum shift function. In this experiment the shift of the time-integrated SPE echo maximum is measured with respect to $t_{12} = 0$ at a particular waiting time t_{13}, when the delay time t_{12} is scanned (Fig. 2). The observed quantum beats are caused by the coupling of the optical transition to several vibrational modes.

Figure 3 compares the results obtained for time-integrated versus diagonal time-gated photon echo experiments. In the time-integrated echo detection technique the echo decays are virtually independent of whether the third pulse is in or out of phase with the rephasing wave packet. In striking contrast, in the time-gated case the echo decays are found to be strongly dependent on the timing of the third pulse. For $t_{13} = 210$ fs, where maximal mode suppression is expected, the echo signal can be measured up to $t_{12} = 100$ fs. In the Markovian limit the echo decay corresponds to an optical dephasing time T_2 of ~35 fs. The fact that the integrated echo signal exhibits no signature of mode suppression, proves how-

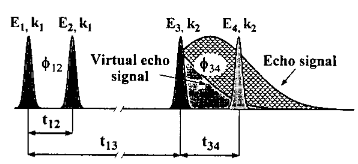

QThA3 Fig. 1 Pulse sequence in PL-HSPE experiment. ϕ_{12} and ϕ_{34} denote the relative phases between pulses E_1-E_2 and E_3-E_4, respectively, while k_1 and k_2 stand for their wave vectors. Conventional rephasing echo as well as nonrephasing virtual echo contributions to the total signal are depicted. 13-fs laser pulses were used for all experiments.

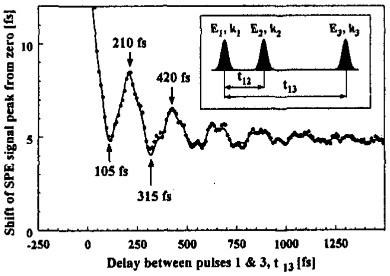

QThA3 **Fig. 2** Echo-shift from zero (●) as a function for the waiting time t_{13}. The inset shows the pulse sequence used in this experiment. Arrows indicate the turning points of the vibrational wave-packet motion.

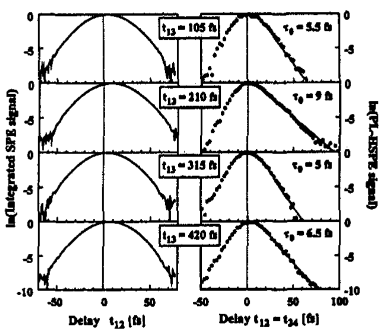

QThA3 **Fig. 3** Mode suppression in time-integrated (left panel) versus time-gated (right panel) photon echo experiments. For the time-gated signals, the conventional rephasing contribution and nonrephasing virtual echoes are shown at positive and negative times, respectively, for comparison. Fits to time-gated signals by a linear function $-t_{12}/\tau_0$ are also shown (right panel, solid curves).

ever that the system dynamics are non-Markovian. The observed exponential decay of the SPE for t_{13} = 210 fs thus necessitates the presence of an ultrafast non-Markovian process, whose correlation time is much less than 200 fs. For third-pulse delays getting longer the time-gated echo decays become increasingly faster because of the decay time of the vibrational coherence (~350 fs).

Compared with the sophistication of multiple-pulse NMR, multiple-pulse optical experiments have a long way to go. In particular, it still remains a formidable challenge to suppress not only a single vibrational mode, but all of them in an echo decay.

1. R. W. Schoenlein, D. M. Mittleman, J. J. Shiang, A. P. Alivisatos, C. V. Shank, Phys. Rev. Lett. **70**, 1014 (1993); C. J. Bardeen, C. V. Shank, Chem. Phys. Lett. **203**, 535 (1993); *ibid.* **226**, 310 (1994).
2. M. S. Pshenichnikov, K. Duppen, D. A. Wiersma, Phys. Rev. Lett. **74**, 674 (1995); P. Vöhringer, D. C. Arnett, T.-S. Yang, N. F. Scherer, Chem. Phys. Lett. **237**, 387 (1995).
3. W. P. de Boeij, M. S. Pshenichnikov, D. A. Wiersma, Chem. Phys. Lett. **238**, 1 (1995).
4. M. Cho, N. F. Scherer, G. R. Fleming, S. Mukamel, J. Chem. Phys. **96**, 5618 (1992).

QThA4 **9:15 am**

Memory effects in the momentum orientation relaxation of optically excited plasmas in semiconductors

R. Binder, H. S. Köhler,* M. Bonitz,**
Optical Sciences Center, University of Arizona, Tucson, Arizona 85721

Optical excitation of electron-hole plasma in semiconductor yields, in general, anisotropic momentum distributions of the excited charge carriers. It is well known that, even in bulk III-V semiconductors such as GaAs, optical excitation creates anisotropic plasmas resulting from the effects of spin orbit interaction. The initial anisotropy of the excited conduction band electrons is different for the contribution resulting from excitation from the heavy-hole valence band and that of the light-hole valence band. The momentum orientation relaxation, *i.e.*, the scattering processes that make the distribution of carriers essentially isotropic, is believed to be the fastest scattering mechanism in semiconductors and essentially solely governed by carrier-carrier scattering.

Recently, the issue of so-called memory effects, *i.e.*, the deviation of relaxation processes from simple Markov processes, has drawn considerable attention. It seems intuitively clear that, if at all, such memory effects should be most important in the fastest relaxation processes. For this reason, we have begun to study memory effects in the momentum orientation relaxation.

The theoretical basis of our analysis are the equations of motion for the the full two-time one-particle Green's function $g<(\vec{k}, t_1, t_2)$ within the screened Hartree–Fock approximation. This Green's function reduces to the distribution function of the charge carriers as function of momentum k and time t in the equal time limit: $f(\vec{k}, t) = -i\hbar g<(\vec{k}, t, t)$. Our numerical solution incorporates full correlation effects because it is based on an time integration in the two-dimensional $t_1 - t_2$ plane. Of course, one can apply certain additional approximations such as the Markov approximation to reduce the equation of motion to the conventional Boltzmann equation. The comparison of the results with and without such additional approximations yields important information about charge-carrier correlation contributions, memory effects, and nonkinetic energy preserving processes.

The two-time approach poses enormous numerical challenges. For this reason, we have thus far limited our investigations to the following situation. Instead of treating the optical excitation process dynamically, we solve only the initial value problem for the electron distribution. Also, we have considered only electron-electron scattering. Screening of the Coulomb potential is treated within a simple quasi-static model. Although we intend to improve our model in all of

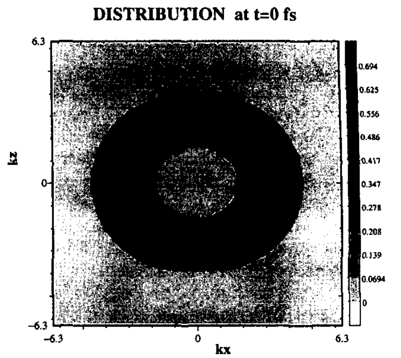

QThA4 **Fig. 1** Initial charge-carrier distribution as function of momentum vector $\vec{k}$. The distribution shown is for $k_y = 0$. The distribution in three-dimensional momentum space is obtained from this figure by rotating around the z axis.

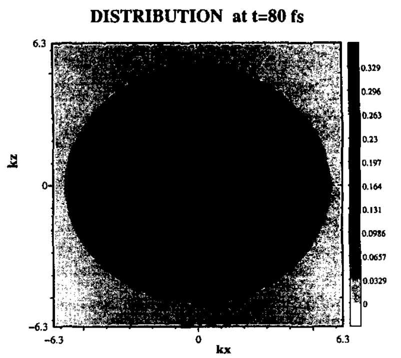

QThA4 **Fig. 2** Same as Fig. 1 but after 80 fs, calculated with full two-time Green's function method.

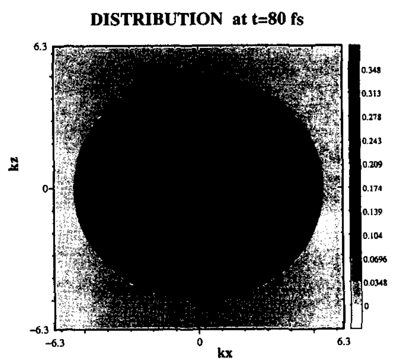

QThA4 **Fig. 3** Same as Fig. 2 but within the approximation of the conventional Boltzmann equation without any memory effects.